Adaptive Reciprocal-Kind Zeroing Neural Network Solving Temporally Dependent Quadratic Programming with Application to Robotic Arms

Journal:	*IEEE Transactions on Neural Networks and Learning Systems*
Manuscript ID	TNNLS-2022-P-25675
Manuscript Type:	Regular Paper
Date Submitted by the Author:	21-Dec-2022
Complete List of Authors:	Guo, Pengfei; Zhongkai University of Agriculture and Engineering, School of Computational Science Zhang, Yunong; Sun Yat-Sen University, School of Computer Science and Engineering Li, Shuai; Swansea University, Faculty of Science and Engineering
Keywords:	Temporally dependent quadratic programming, adaptive reciprocal-kind zeroing neural network (ARKZNN), Lyapunov stability, robot arm

Adaptive Reciprocal-Kind Zeroing Neural Network Solving Temporally Dependent Quadratic Programming with Application to Robotic Arms

Pengfei Guo, *Member, IEEE*, Yunong Zhang, *Member, IEEE*, Shuai Li, *Senior Member, IEEE*

***Abstract*—Temporally dependent quadratic programming (QP) constrained with equality constraint (EC) is regarded as a fundamental problem in artificial intelligence and modern control engineering. Zeroing neural network (ZNN), which is a canonical method, can be adopted to deal with temporally dependent QP problem with EC. In order to overcome the issue of temporally dependent inverse computing, a novel ZNN model, which is termed as adaptive reciprocal-kind zeroing neural network (ARKZNN) model, is proposed by mixing the energy-type cost function and ZNN design formula for solving the temporally dependent QP problem with EC in this paper. The convergence property of reciprocal-kind zeroing neural network (RKZNN) model is obtained by Lyapunov stability theory, while the convergence property of ARKZNN model is analyzed by the limit thinking. Moreover, two numerical experiments are conducted to show the parameters influence, effectiveness and superiority of ARKZNN model for solving temporally dependent QP problem with EC. As an application, a simulation for solving the path-tracking problem of PUMA560 robot arm is performed to illustrate the effectiveness and superiority of our proposed Euler-ARKZNN algorithm.**

***Index Terms*—Temporally dependent quadratic programming, adaptive reciprocal-kind zeroing neural network (ARKZNN), Lyapunov stability, robot arm.**

I. Introduction

QUADRATIC programming (QP) is regarded as a fundamental and important modelling approach in modern information science and artificial intelligence engineering field [1]–[3], which also attracts lots of researchers' attention. For example, many loss functions of deep neural network (DNN) models are formulated as a classical QP optimization problem derived by energy minimization method [4], [5], while the model prediction control (MPC) problem is aimed to optimize a QP constrained with dynamic system and output equation problem [6], [7]. On the basis of optimization and numerical analysis theory, many approaches are proposed for solving static QP problem [8]–[10]. However, as the development of internet of things, many tasks in artificial intelligence and modern control engineering should be finished in real time [11]–[13]. Therefore, we need to develop the online algorithms for solving the temporally dependent QP problem.

Traditionally, the temporally dependent QP problem is divided into static QP subproblems by sampling method that can be solved through classical optimization approaches [14], [15]. However, when the temporally dependent QP problem is divided into static QP subproblems, the important connection information inspired by temporally continuous property is largely reduced, and the precision of those models highly relates with the sampling method. As the development of neural network theory, the neurodynamic-inspired recurrent neural network (RNN) models are constructed by related design formulas (e.g., Zhang design formula and gradient design formula) to solve temporally dependent optimization problem and nonlinear control problem [16]–[19], which can specially solve the problem of various temporally dependent QP [20]–[23].

In last two decades, zeroing neural network (ZNN) model [24], which is a canonical type of RNN method, has been adopted to solve the problem of temporally dependent QP with EC. In 2009, Zhang et al. firstly constructed the ZNN model for solving the temporally dependent QP problem with equality constraints (EC), and the numerical experiments showed the good efficacy of ZNN solver compared with gradient neural network (GNN) solver [25]. In 2013, Yang et al. proposed a more robust ZNN model activated by the power-sum activation functions to solve the temporally dependent QP problem with EC perturbed by large implementation errors [26]. In 2018, Xiao et al. presented a versatile ZNN (VZNN) model by designing a pair of parameters and activation functions, which is of noise-tolerance and finite-time convergence, for solving the temporally dependent QP problem [27]. In 2019, Zhang et al. gave a framework of varying parameter ZNN (VPZNN) model for solving the temporally dependent QP problem with EC or inequality constraints (IEC) by designing the model parameter as a temporally dependent function, which made the residual error vector converge to zero vector with a super-exponential convergence rate [28]. In view of different number domains, Qi et al. proposed a complex-valued ZNN (CVZNN) model to solve the problem of perturbed

The work is supported by the National Natural Science Foundation of China (with number 61976230), the Project Supported by Guangdong Province Universities and Colleges Pearl River Scholar Funded Scheme (with number 2018), the Key-Area Research and Development Program of Guangzhou (with number 202007030004), the Guangdong Basic and Applied Basic Research Foundation (with number 2020A1515110958), and also the Research Fund Program of Guangdong Key Laboratory of Modern Control Technology (with number 2017B030314165).

P. Guo is with the School of Computational Science, Zhongkai University of Agriculture and Engineering, Guangzhou, 510115, China, and with the School of Computer Science and Engineering, Sun Yat-sen University, Guangzhou 510006, China.

Y. Zhang is with the School of Computer Science and Engineering, Sun Yat-sen University, Guangzhou 510006, China, e-mail: zhynong@mail.sysu.edu.cn (corresponding author).

S. Li is with the Faculty of Science and Engineering, and also affiliated to Zienkiewicz Centre for Computational Engineering, Swansea University, Swansea SA18EN, U.K., shuai.li@swansea.ac.uk.

complex temporally dependent QP with EC [29]. In 2021, Jia et al. developed an adaptive fuzzy ZNN (AFZNN) model for solving the temporally dependent QP problem with EC to adjust the temporally dependent convergence rate on the basis of computational residual errors [30]. Recently, Zhang et al. integrated the VPZNN model and Karush-Kuhn-Tucker (KKT) conditions to design a barrier VPZNN (BVPZNN) model for solving the temporally dependent QP problem with EC, IEC, and bound conditions [31].

From the above literatures, we can see that the ZNN model and its variants can be used to obtain the theoretical solution of the problem of the temporally dependent QP. However, these models are expressed in the implicit form, or the explicit form adopted temporally dependent inverse matrix or pseudo-inverse matrix. The implicit form models are hard to implement in the real world application, while the explicit form models suffer the high-complexity temporally dependent inverse or pseudo-inverse computing problem. Although some researchers have developed a cascade system with two subsystems, which included a ZNN model for temporally dependent inverse computing and a ZNN model for solving the temporally dependent QP problem [32], it is ready to see there is an obvious efficient obstacle. Therefore, some single inverse-free ZNN models should be developed to solve the problem of the temporally dependent QP.

In this paper, in order to overcome the temporally dependent inverse computing problem and inspired by the GNN model, a novel single inverse-free ZNN model, which is termed as adaptive reciprocal-kind zeroing neural network (ARKZNN) model, is proposed by mixing the 2-norm energy cost function and ZNN design formula for solving temporally dependent QP problem with EC. The convergence property related with model parameters of reciprocal-kind zeroing neural network (RKZNN) and ARKZNN is obtained by Lyapunov stability theory and the limit thinking. Moreover, two numerical experiments are conducted to show the effectiveness and superiority of ARKZNN model for solving temporally dependent QP problem with EC. Finally, the discrete form of the ARKZNN model, which is named as Euler-ARKZNN algorithm, is adopted to solve the problem of robot arm path-tracking. The main contributions are listed as follows.

- An AKRZNN model, which is a single inverse-free ZNN model, is constructed to solve the problem of temporally dependent QP with EC.
- The convergence property of RKZNN and ARKZNN is obtained by Lyapunov stability theory and the limit thinking, and the parts effects of derivative feedforward and proportional feedback are evidently described by Lyapunov stability theory and matrix spectral theory.
- Two numerical experiments are conducted to show the model parameters influence, effectiveness, and superiority of ARKZNN model for solving the temporally dependent QP problem with EC.
- One simulation is conducted to show the effectiveness and superiority of the Euler-ARKZNN algorithm for solving the robot arm path-tracking problem.

The remainder content of this paper is organized as following. In Section II, we formulate the temporally dependent QP problem with EC. In Section III, we give the framework of ARKZNN model and the compared state-of-the-art models for solving the temporally dependent QP problem with EC. In Section IV, we discuss the convergence property of ARKZNN model. In Section V, we show the results of related numerical experiments of ARKZNN model. In Section VI, we apply the Euler-ARKZNN algorithm to robot arm control. We conclude the paper in Section VII.

II. Problem Formulation

In this section, we formulate the temporally dependent QP problem with EC.

In real world applications, lots of dynamic engineering problems can be solved by minimal energy method, which are formulated as the following temporally dependent QP problem with EC by reducing the observed related term:

$$\begin{aligned} &\min_{\mathbf{x}(t)} \; \mathbf{x}^{\mathrm{T}}(t)\mathcal{Q}(t)\mathbf{x}(t) + \boldsymbol{\varrho}^{\mathrm{T}}(t)\mathbf{x}(t), \\ &\text{s.t. } \mathcal{A}(t)\mathbf{x}(t) = \mathbf{b}(t), \end{aligned} \tag{1}$$

where $\mathbf{x}(t)$ is the unknown vector at time instant $t \in [0, T)$, T is the terminal time, $\mathcal{Q}(t) \in \mathbb{R}^{n\times n}$ is a semi-definite positive temporally continuous matrix, $\mathcal{A}(t) \in \mathbb{R}^{m\times n}$ is an observable information matrix, $\boldsymbol{\varrho}(t) \in \mathbb{R}^{n\times 1}$ and $\mathbf{b}(t) \in \mathbb{R}^{m\times 1}$ are observable information vectors, and $[\cdot]^{\mathrm{T}}$ is the transpose matrix of input-matrix argument. In this paper, we suppose that all observable matrices $\mathcal{Q}(t), \mathcal{A}(t)$ and vectors $\boldsymbol{\varrho}(t), \mathbf{b}(t)$ are order-2 differentiable. Due to the temporally related property, the targeted unknown vector $\mathbf{x}(t)$ should have more flexible differential property.

III. Proposed Method

In this section, we present the RKZNN and ARKZNN models for solving the temporally dependent QP problem with EC (1) by ZNN theory. In addition, we also propose an Euler-ARKZNN algorithm for solving the future QP (FQP) with EC problem.

A. Proposed RKZNN Model and ARKZNN Model

On the basis of the Lagrange multiplier approaches for multi-dimensional optimization problem, we constructed the following Lagrangian for solving the temporally dependent QP problem with EC (1):

$$\mathcal{L}(t) = \mathbf{x}^{\mathrm{T}}(t)\mathcal{Q}(t)\mathbf{x}(t) + \boldsymbol{\varrho}^{\mathrm{T}}(t)\mathbf{x}(t) + \boldsymbol{\lambda}^{\mathrm{T}}(t)(\mathcal{A}(t)\mathbf{x}(t) - \mathbf{b}(t)), \tag{2}$$

where $\boldsymbol{\lambda}(t) \in \mathbb{R}^{m\times 1}$ is the Lagrange multiplier parameter vector. Then, due to the differentiable property of $\mathcal{L}(t)$, the extremum of Lagrangian (2) should satisfy the following linear system that is obtained by partially differentiating $\mathcal{L}(t)$ with respect to $\mathbf{x}(t)$ and $\boldsymbol{\lambda}(t)$:

$$\begin{cases} \nabla_{\mathbf{x}(t)}\mathcal{L}(t) = \mathcal{Q}(t)\mathbf{x}(t) + \mathcal{A}^{\mathrm{T}}(t)\boldsymbol{\lambda}(t) + \boldsymbol{\varrho}(t) = \mathbf{0}, \\ \nabla_{\boldsymbol{\lambda}(t)}\mathcal{L}(t) = \mathcal{A}(t)\mathbf{x}(t) - \mathbf{b}(t) = \mathbf{0}. \end{cases} \tag{3}$$

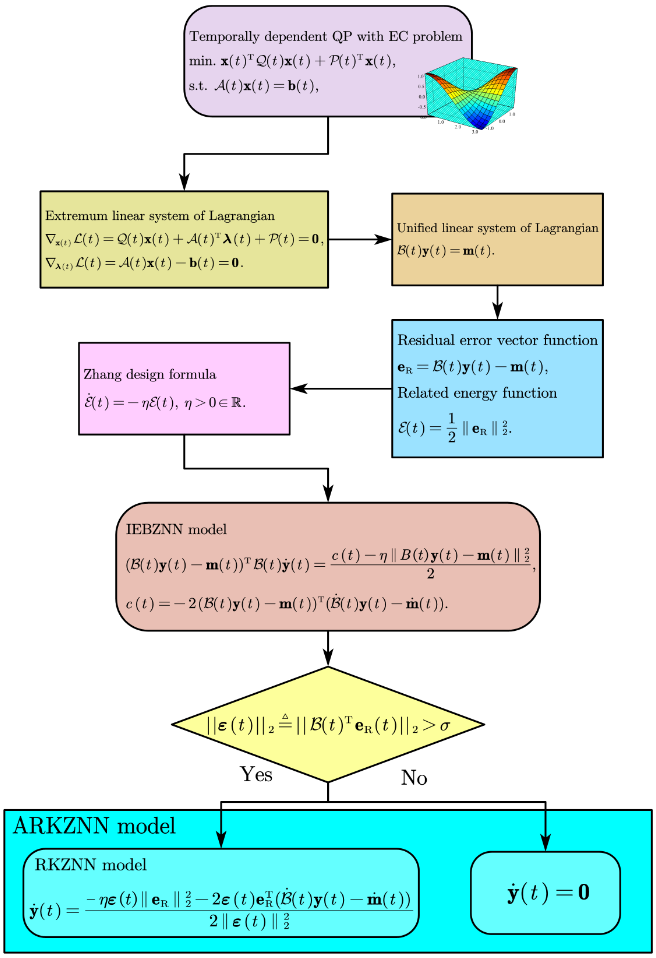

Fig. 1. Flowchart of ARKZNN model for solving temporally dependent QP problem with EC (1).

This extremum linear system (3) is reformulated as the following unified linear system:

$$\mathcal{B}(t)\mathbf{y}(t)=\mathbf{m}(t), \tag{4}$$

where

$$\mathcal{B}(t)=\begin{bmatrix}\mathcal{Q}(t) & \mathcal{A}^{\mathrm{T}}(t)\\ \mathcal{A}(t) & O\end{bmatrix}, \mathbf{y}(t)=\begin{bmatrix}\mathbf{x}(t)\\ \boldsymbol{\lambda}(t)\end{bmatrix}, \mathbf{m}(t)=\begin{bmatrix}-\boldsymbol{\varrho}(t)\\ \mathbf{b}(t)\end{bmatrix}.$$

Then, the temporally dependent QP problem with EC (1) is solved by finding the temporally dependent solution $\mathbf{y}(t)$ of unified linear system (4). In order to find the solution of (4), we define a residual error vector function $\mathbf{e}_{\mathrm{R}}(t)=\mathcal{B}(t)\mathbf{y}(t)-\mathbf{m}(t)$, and the related energy function is defined as $\mathcal{E}(t)=\|\mathbf{e}_{\mathrm{R}}(t)\|_2^2/2$, where $\|\cdot\|_2$ denotes the 2-norm of input vector augment. The Zhang design formula $\dot{\mathcal{E}}(t)=-\eta\mathcal{E}(t)$ is adopted to construct the following implicit energy-based ZNN (IEBZNN) model for solving the temporally dependent QP problem with EC (1):

$$\begin{aligned}&(\mathcal{B}(t)\mathbf{y}(t)-\mathbf{m}^{\mathrm{T}}(t))\mathcal{B}(t)\dot{\mathbf{y}}(t)\\ =&-(\mathcal{B}(t)\mathbf{y}(t)-\mathbf{m}^{\mathrm{T}}(t))\dot{\mathcal{B}}(t)\mathbf{y}(t)-\frac{\eta\|\mathcal{B}(t)\mathbf{y}(t)-\mathbf{m}(t)\|_2^2}{2}\\ &+(\mathcal{B}(t)\mathbf{y}(t)-\mathbf{m}^{\mathrm{T}}(t))\dot{\mathbf{m}}(t),\end{aligned} \tag{5}$$

where $\eta\in\mathbb{R}^{+}$ is the IEBZNN design parameter. From above equation, we can see that the IEBZNN model (5) is a scalar-scale mathematical modelling, which is common in lots of machine learning algorithms. Furthermore, the IEBZNN model (5) can be simplified as the following form by residual error vector function $\mathbf{e}_{\mathrm{R}}(t)$:

$$\mathbf{e}_{\mathrm{R}}^{\mathrm{T}}(t)\mathcal{B}(t)\dot{\mathbf{y}}(t)=-\frac{\eta}{2}\|\mathbf{e}_{\mathrm{R}}(t)\|_2^2-\mathbf{e}_{\mathrm{R}}^{\mathrm{T}}(t)(\dot{\mathcal{B}}(t)\mathbf{y}(t)-\dot{\mathbf{m}}(t)). \tag{6}$$

We denote the gradient of related energy function $\mathcal{E}(t)$ with respect to residual error vector $\mathbf{e}_{\mathrm{R}}(t)$ as $\boldsymbol{\varepsilon}(t)$, i.e., $\boldsymbol{\varepsilon}(t)\triangleq\nabla_{\mathbf{e}_{\mathrm{R}}(t)}\mathcal{E}(t)=\mathcal{B}^{\mathrm{T}}(t)\mathbf{e}_{\mathrm{R}}(t)$. Then, we obtain the following explicit energy-based ZNN model for solving the temporally dependent QP problem with EC (1), which is termed as reciprocal-kind zeroing neural network (RKZNN) model:

$$\dot{\mathbf{y}}(t)=\frac{-\eta\boldsymbol{\varepsilon}(t)\|\mathbf{e}_{\mathrm{R}}(t)\|_2^2-2\boldsymbol{\varepsilon}(t)\mathbf{e}_{\mathrm{R}}^{\mathrm{T}}(t)(\dot{\mathcal{B}}(t)\mathbf{y}(t)-\dot{\mathbf{m}}(t))}{2\|\boldsymbol{\varepsilon}(t)\|_2^2}. \tag{7}$$

It is important to note that the RKZNN model (7) is a vector-scale mathematical modelling, which shares the same element-wise convergence property with the universal ZNN model framework. In order to overcome the denominator vanishing problem, the RKZNN model (7) for solving the temporally dependent QP problem with EC (1) is filtered into the following ARKZNN model by any rigid threshold $\sigma\in\mathbb{R}^{+}$:

$$\dot{\mathbf{y}}(t)=\begin{cases}\frac{-\eta\boldsymbol{\varepsilon}(t)\|\mathbf{e}_{\mathrm{R}}(t)\|_2^2-2\boldsymbol{\varepsilon}(t)\mathbf{e}_{\mathrm{R}}^{\mathrm{T}}(t)(\dot{\mathcal{B}}(t)\mathbf{y}(t)-\dot{\mathbf{m}}(t))}{2\|\boldsymbol{\varepsilon}(t)\|_2^2}, & \text{if } \|\boldsymbol{\varepsilon}(t)\|_2>\sigma,\\ \mathbf{0}, & \text{otherwise.}\end{cases} \tag{8}$$

Remark 1: In this paper, we construct a novel ZNN model (ARKZNN model) for solving the temporally dependent QP problem with EC (1) by using a scalar energy error function, while the classical ZNN model and its variants are developed by adopting a vector error function. In order to better understand the ARKZNN model, we illustrate its constructing process in Fig. 1. Usually, when we adopt the classical ZNN model and its variants to solve the temporally dependent QP problem with EC (1), the temporally dependent matrix inverse computing is an unavoidable problem. However, from Fig. 1, we can see that the proposed RKZNN model (7) and ARKZNN model (8) are total inverse-free neurodynamic models. That is to say, the proposed RKZNN model (7) and ARKZNN model (8) have superiority on modelling form and computation complexity parts, comparing with the classical ZNN model and its variants.

Remark 2: The proposed RKZNN model (7) for solving the temporally dependent QP problem with EC (1) is constructed by Zhang design formula, which is equivalent to the proportion derivative (PD) feedback control method. Specifically, the first term of numerator of RKZNN model (7) in right side represents proportion feedback (PF), while the second term of numerator of RKZNN model (7) in right side represents derivative feedforward (DF). We visualize the RKZNN model (7) for solving the temporally dependent QP problem with EC (1) by block diagram in Fig. (2). In addition, the ARKZNN model without PF is formulated as follows:

$$\dot{\mathbf{y}}(t)=\begin{cases}-\dfrac{\boldsymbol{\varepsilon}(t)\mathbf{e}_{\mathrm{R}}^{\mathrm{T}}(t)(\dot{\mathcal{B}}(t)\mathbf{y}(t)-\dot{\mathbf{m}}(t))}{\|\boldsymbol{\varepsilon}(t)\|_2^2}, & \text{if } \|\boldsymbol{\varepsilon}(t)\|_2>\sigma,\\ \mathbf{0}, & \text{otherwise.}\end{cases} \tag{9}$$

while the ARKZNN model without DF is formulated as follows:

$$\dot{\mathbf{y}}(t)=\begin{cases}-\dfrac{\eta\boldsymbol{\varepsilon}(t)\|\mathbf{e}_{\mathrm{R}}(t)\|_2^2}{2\|\boldsymbol{\varepsilon}(t)\|_2^2}, & \text{if } \|\boldsymbol{\varepsilon}(t)\|_2>\sigma,\\ \mathbf{0}, & \text{otherwise.}\end{cases} \tag{10}$$

These two models are presented to do related ablation experiments of the ARKZNN model (8) for solving the temporally dependent QP problem with EC (1).

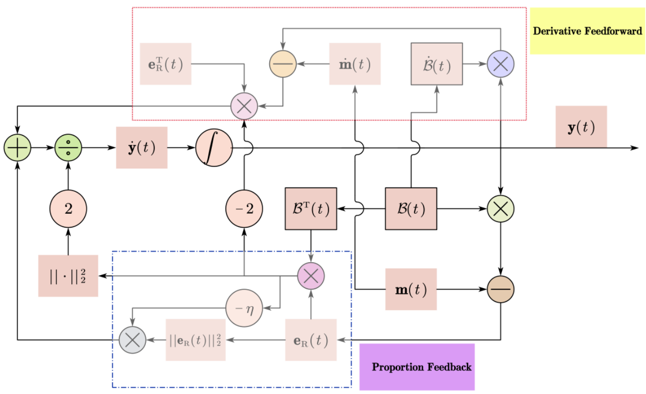

Fig. 2. Block diagram of RKZNN model (7) for solving temporally dependent QP problem with EC (1).

Remark 3: As the high complexity of temporally dependent matrix inverse computing, we focus on the inverse-free model for solving the temporally dependent QP problem with EC (1) in this paper. In order to show the superiority of our proposed ARKZNN model, we list three types of RNN models for solving the temporally dependent QP problem with EC (1). The first one is an explicit energy based gradient neural network (EEBGNN) model that is obtained by gradient design formula $\dot{\mathbf{y}}(t)=-\kappa\nabla_{\mathbf{y}(t)}\mathcal{E}(t)$, where $\kappa>0\in\mathbb{R}$ is the EEBGNN model parameter. The EEBGNN model for solving the temporally dependent QP problem with EC (1) is formulated as follows:

$$\dot{\mathbf{y}}(t)=-\kappa\mathcal{B}^{\mathrm{T}}(t)(\mathcal{B}(t)\mathbf{y}(t)-\mathbf{m}(t)). \tag{11}$$

The second one is a hybrid gradient ZNN (HGZNN) model, which adopts the Getz-Marsden dynamic system (GMDS) model 2 for the temporally dependent inverse computing. The HGZNN model for solving the temporally dependent QP problem with EC (1) is formulated as follows:

$$\begin{cases}\dot{X}(t)=-X(t)\dot{\mathcal{B}}(t)X(t)-\gamma\mathcal{B}^{\mathrm{T}}(t)(\mathcal{B}(t)X(t)-I),\\ \dot{\mathbf{y}}(t)=-X(t)(\dot{\mathcal{B}}(t)\mathbf{y}(t)-\dot{\mathbf{m}}(t)-\dfrac{\upsilon}{2}t^3(\mathcal{B}(t)\mathbf{y}(t)-\mathbf{m}(t))),\end{cases} \tag{12}$$

where $\gamma\in\mathbb{R}^+$ is the design parameter of GMDS model 2 for the temporally dependent inverse computing, υ is the design parameter of parameter-varying ZNN model for solving the temporally dependent QP problem with EC (1), and $I\in\mathbb{R}^{(m+n)\times(m+n)}$ is the identity matrix. The third one is a gradient-zeroing neural network (GZNN) model, which integrates the advantages of GNN and ZNN models formed a partial inverse-free RNN model. The GZNN model for solving the temporally dependent QP problem with EC (1) is formulated as follows:

$$\begin{aligned}\dot{\mathbf{y}}(t)=&-\mathcal{B}^{-1}(t)(\dot{\mathcal{B}}(t)\mathbf{y}(t)-\dot{\mathbf{m}}(t))\\&-\kappa\mathcal{B}^{\mathrm{T}}(t)((\mathcal{B}(t)\mathbf{y}(t)-\mathbf{m}(t))),\end{aligned} \tag{13}$$

where $\kappa\in\mathbb{R}^+$ is the EEBGNN model parameter.

B. Proposed Euler-ARKZNN Algorithm

In this subsection, we present the Euler-ARKZNN algorithm, which is a discrete form of the ARKZNN model (8), for solving the discrete temporally dependent QP problem with EC.

The temporally dependent QP problem with EC (1) is always expressed as its discrete form in real world applications (e.g., robot arm path-tracking), which is also termed as FQP with EC problem. Let $\mathbf{x}_{k+1},\mathbf{b}_{k+1},\boldsymbol{\varrho}_{k+1},\mathcal{A}_{k+1}$, and $\mathcal{Q}_{k+1}$ be the corresponding vectors and matrices to be sampled at the time instant $(k+1)g$, where g is the sampling gap. Then, the FQP with EC problem is expressed as the follows:

$$\begin{aligned}\min_{\mathbf{x}_{k+1}}.\ &\mathbf{x}_{k+1}^{\mathrm{T}}\mathcal{Q}_{k+1}\mathbf{x}_{k+1}+\boldsymbol{\varrho}_{k+1}^{\mathrm{T}}\mathbf{x}_{k+1},\\ \text{s.t. }&\mathcal{A}_{k+1}\mathbf{x}_{k+1}=\mathbf{b}_{k+1},\end{aligned} \tag{14}$$

where $\mathbf{x}_{k+1}$ should be obtained without using any information at the time instant $(k+1)g$.

Let

$$\mathcal{B}_k=\begin{bmatrix}\mathcal{Q}_k & \mathcal{A}_k^{\mathrm{T}}\\ \mathcal{A}_k & O\end{bmatrix},\mathbf{y}_k=\begin{bmatrix}\mathbf{x}_k\\ \boldsymbol{\lambda}_{k+1}\end{bmatrix},\mathbf{m}_k=\begin{bmatrix}-\boldsymbol{\varrho}_k\\ \mathbf{b}_k\end{bmatrix},$$

$\mathbf{e}_{\mathrm{R},k}=\mathcal{B}_k\mathbf{y}_k-\mathbf{m}_k$, and $\boldsymbol{\varepsilon}_k=\mathcal{B}_k^{\mathrm{T}}\mathbf{e}_{\mathrm{R},k}$. On the basis of Zhang time discretization theory, the Euler-ARKZNN algorithm for solving the FQP with EC problem (14), which is combined the Euler forward formula and the ARKZNN model (8), is formulated as follows:

- If $\|\boldsymbol{\varepsilon}_k\|_2>\sigma$, then

$$\mathbf{y}_{k+1}=\mathbf{y}_k-g\frac{\eta\boldsymbol{\varepsilon}_k\|\mathbf{e}_{\mathrm{R},k}\|_2^2+2\boldsymbol{\varepsilon}_k\mathbf{e}_{\mathrm{R},k}^{\mathrm{T}}(\dot{\mathcal{B}}_k\mathbf{y}_k-\dot{\mathbf{m}}_k)}{2\|\boldsymbol{\varepsilon}_k\|_2^2}. \tag{15}$$

- If $\|\boldsymbol{\varepsilon}_k\|_2\le\sigma$, then

$$\mathbf{y}_{k+1}=\mathbf{y}_k. \tag{16}$$

The Euler-ARKZNN algorithm (15) and (16) for solving the FQP with EC problem (14) is proposed to tackle the path-tracking problem of PUMA560 robot arm. As a comparison, we formulate the Euler-EEBGNN algorithm as follows:

$$\mathbf{y}_{k+1}=\mathbf{y}_k-g\kappa\mathcal{B}_k^{\mathrm{T}}(\mathcal{B}_k\mathbf{y}_k-\mathbf{m}_k). \tag{17}$$

IV. Convergence Analyse

In this section, we present the convergence analyses of RKZNN model (7) and ARKZNN model (8) by Lyapunov stability theory and the limit thinking for solving the temporally dependent QP problem with EC (1).

Let the solution error $\mathbf{e}_{\mathrm{S}}(t) = \mathbf{y}(t) - \mathbf{y}^*(t)$, where $\mathbf{y}^*(t)$ is the theoretical solution of unified linear system (4). We present the convergence property of RKZNN model (7) for solving the temporally dependent QP problem with EC (1).

Theorem 1: Suppose that the temporally dependent matrix $\mathcal{B}(t)$ is differentiable with order-2, and the temporally dependent $\mathbf{m}(t)$ is differentiable with order-2. Starting with initial vector $\mathbf{y}(0)$, the RKZNN model (7) continuously, exponentially, and globally converges to the theoretical solution $\mathbf{y}^*(t)$ of unified linear system (4) with exponential rate $\eta/2$, which further gives the theoretical solution $\mathbf{x}^*(t)$ of the temporally dependent QP problem with EC (1).

Proof. Assume that $\mathbf{y}^*(t)$ is the theoretical solution of unified linear system (4), that is, $\mathcal{B}(t)\mathbf{y}^*(t) = \mathbf{m}(t)$. In order to obtain the convergence property of RKZNN model (7), we define the related residual error based Lyapunov candidate function as $\mathcal{V}(t) = \|\mathbf{e}_{\mathrm{R}}(t)\|_2^2/2$, which is a positive-definite bilinear temporally dependent function. Then, the derivative of Lyapunov candidate function $\mathcal{V}(t)$ is computed as follows:

$$\begin{aligned}
\dot{\mathcal{V}}(t) =& \frac{\mathrm{d}}{\mathrm{d}t}\left(\frac{\|\mathbf{e}_{\mathrm{R}}(t)\|_2^2}{2}\right)\\
=&\mathbf{e}_{\mathrm{R}}^{\mathrm{T}}(t)\dot{\mathbf{e}}_{\mathrm{R}}(t)\\
=&\mathbf{e}_{\mathrm{R}}^{\mathrm{T}}(t)(\dot{\mathcal{B}}(t)\mathbf{y}(t) + \mathcal{B}(t)\dot{\mathbf{y}}(t) - \dot{\mathbf{m}}(t))\\
=&\mathbf{e}_{\mathrm{R}}^{\mathrm{T}}(t)\Big(\dot{\mathcal{B}}(t)\mathbf{y}(t) - \dot{\mathbf{m}}(t) - \mathcal{B}(t)\frac{\eta\boldsymbol{\varepsilon}(t)\|\mathbf{e}_{\mathrm{R}}(t)\|_2^2}{2\|\boldsymbol{\varepsilon}(t)\|_2^2}\\
&- \mathcal{B}(t)\frac{\boldsymbol{\varepsilon}(t)\mathbf{e}_{\mathrm{R}}^{\mathrm{T}}(t)(\dot{\mathcal{B}}(t)\mathbf{y}(t) - \dot{\mathbf{m}}(t))}{\|\boldsymbol{\varepsilon}(t)\|_2^2}\Big)\\
=&\mathbf{e}_{\mathrm{R}}^{\mathrm{T}}(t)(\dot{\mathcal{B}}(t)\mathbf{y}(t) - \dot{\mathbf{m}}(t)) - \eta\frac{\boldsymbol{\varepsilon}^{\mathrm{T}}(t)\boldsymbol{\varepsilon}(t)\|\mathbf{e}_{\mathrm{R}}(t)\|_2^2}{2\|\boldsymbol{\varepsilon}(t)\|_2^2}\\
&- \frac{\boldsymbol{\varepsilon}^{\mathrm{T}}(t)\boldsymbol{\varepsilon}(t)\mathbf{e}_{\mathrm{R}}^{\mathrm{T}}(t)(\dot{\mathcal{B}}(t)\mathbf{y}(t) - \dot{\mathbf{m}}(t))}{\|\boldsymbol{\varepsilon}(t)\|_2^2}\\
=&\mathbf{e}_{\mathrm{R}}^{\mathrm{T}}(t)(\dot{\mathcal{B}}(t)\mathbf{y}(t) - \dot{\mathbf{m}}(t)) - \eta\frac{\|\boldsymbol{\varepsilon}(t)\|_2^2\|\mathbf{e}_{\mathrm{R}}(t)\|_2^2}{2\|\boldsymbol{\varepsilon}(t)\|_2^2}\\
&- \frac{\|\boldsymbol{\varepsilon}(t)\|_2^2\mathbf{e}_{\mathrm{R}}^{\mathrm{T}}(t)(\dot{\mathcal{B}}(t)\mathbf{y}(t) - \dot{\mathbf{m}}(t))}{\|\boldsymbol{\varepsilon}(t)\|_2^2}\\
=& - \eta\frac{\|\mathbf{e}_{\mathrm{R}}(t)\|_2^2}{2} = -\eta\mathcal{V}(t).
\end{aligned} \tag{18}$$

That is to say, the Lyapunov candidate function $\mathcal{V}(t)$ satisfies the following ordinary derivative equation by (18):

$$\dot{\mathcal{V}}(t) = -\eta\mathcal{V}(t).$$

Then, the Lyapunov candidate function $\mathcal{V}(t)$ is formulated as the following explicit form:

$$\mathcal{V}(t) = \mathcal{V}(0)\exp(-\eta t). \tag{19}$$

Substituting $\mathcal{V}(t) = \|\mathbf{e}_{\mathrm{R}}(t)\|_2^2/2$ into (19), we obtain the explicit form of the L_2 norm of residual error $\mathbf{e}_{\mathrm{R}}(t)$:

$$\|\mathbf{e}_{\mathrm{R}}(t)\|_2 = \|\mathbf{e}_{\mathrm{R}}(0)\|_2\exp\left(-\frac{\eta}{2}t\right). \tag{20}$$

The relation of residual error $\mathbf{e}_{\mathrm{R}}(t)$ and solution error $\mathbf{e}_{\mathrm{S}}(t)$ is formulated as $\mathbf{e}_{\mathrm{R}}(t) = \mathcal{B}(t)\mathbf{y}(t) - \mathbf{m}(t) = \mathcal{B}(t)\mathbf{y}(t) - \mathcal{B}(t)\mathbf{y}^*(t) = \mathcal{B}(t)\mathbf{e}_{\mathrm{S}}(t)$. Let α be the infimum of the set of minimal positive eigenvalues of $\mathcal{B}^{\mathrm{T}}(t)\mathcal{B}(t)$. Then,

$$\begin{aligned}
\alpha\|\mathbf{e}_{\mathrm{S}}(t)\|_2^2 \leq&\mathbf{e}_{\mathrm{S}}(t)^{\mathrm{T}}\mathcal{B}^{\mathrm{T}}(t)\mathcal{B}(t)\mathbf{e}_{\mathrm{S}}(t) = \|\mathcal{B}(t)\mathbf{e}_{\mathrm{S}}(t)\|_2^2\\
=&\|\mathbf{e}_{\mathrm{R}}(t)\|_2^2 = \|\mathbf{e}_{\mathrm{R}}(0)\|_2^2\exp(-\eta t).
\end{aligned} \tag{21}$$

Then, the L_2 norm of residual error $\mathbf{e}_{\mathrm{S}}(t)$ is controlled by the following inequality:

$$\|\mathbf{e}_{\mathrm{S}}(t)\|_2 \leq \frac{1}{\sqrt{\alpha}}\|\mathbf{e}_{\mathrm{R}}(0)\|_2\exp\left(-\frac{\eta}{2}t\right). \tag{22}$$

As time t evolves to positive infinity, we obtain the following inequality by computing the limitation of (22):

$$0 \leq \lim_{t\to\infty}\|\mathbf{e}_{\mathrm{S}}(t)\|_2 \leq \lim_{t\to\infty}\frac{1}{\sqrt{\alpha}}\|\mathbf{e}_{\mathrm{R}}(0)\|_2\exp\left(-\frac{\eta}{2}t\right) = 0.$$

Then, $\lim_{t\to\infty}\|\mathbf{e}_{\mathrm{S}}(t)\|_2 = 0$, which means that the RKZNN model (7) continuously, exponentially, and globally converges to the theoretical solution $\mathbf{y}^*(t) = \left[\mathbf{x}^{*\mathrm{T}}(t) \quad \boldsymbol{\lambda}^{*\mathrm{T}}(t)\right]^{\mathrm{T}}$ of unified linear system (4) with exponential rate $\eta/2$, which further gives the theoretical solution $\mathbf{x}^*(t)$ of the temporally dependent QP problem with EC (1). □

On the basis of the convergence property of RKZNN model (7), for any rigid threshold $\sigma > 0$, we present its corresponding finite convergence time property of ARKZNN model (8) for solving the temporally dependent QP problem with EC (1) in the following theorem.

Theorem 2: Suppose that the temporally dependent matrix $\mathcal{B}(t)$ is differentiable with order-2 and satisfies $\|\mathcal{B}(t)\|_{\mathrm{F}} \leq \delta$, and the temporally dependent $\mathbf{m}(t)$ is differentiable with order-2. Starting with initial vector $\mathbf{y}(0)$ and any $\sigma > 0$, the L_2 norm of solution error $\mathbf{e}_{\mathrm{S}}(t)$ of RKZNN model (7) continuously, exponentially and globally converges to the upper bounded σ/δ^2 for unified linear system (4) with exponential rate $\eta/2$, and the convergence time is less than $2\ln(\delta^2\|\mathbf{e}_{\mathrm{R}}(0)\|_2/\sigma\sqrt{\alpha})/\eta$. Furthermore, the ARKZNN model (8) is finite time bounded convergent to the theoretical solution $\mathbf{y}^*(t)$ of unified linear system (4), which also approximates the theoretical solution $\mathbf{x}^*(t)$ of the temporally dependent QP problem with EC (1) in an acceptable range.

Proof. The ARKZNN model (8) is displayed as follows:

$$\dot{\mathbf{y}}(t) = \begin{cases} \frac{-\eta\boldsymbol{\varepsilon}(t)\|\mathbf{e}_{\mathrm{R}}(t)\|_2^2 - 2\boldsymbol{\varepsilon}(t)\mathbf{e}_{\mathrm{R}}^{\mathrm{T}}(t)(\dot{\mathcal{B}}(t)\mathbf{y}(t) - \dot{\mathbf{m}}(t))}{2\|\boldsymbol{\varepsilon}(t)\|_2^2}, & \text{if } \|\boldsymbol{\varepsilon}(t)\|_2 > \sigma,\\ \mathbf{0}, & \text{otherwise.} \end{cases}$$

From rigid threshold condition $\|\boldsymbol{\varepsilon}(t)\|_2 > \sigma$, we obtain the following inequality:

$$\begin{aligned}
\sigma <&\|\boldsymbol{\varepsilon}(t)\|_2 = \|\mathcal{B}^{\mathrm{T}}(t)\mathbf{e}_{\mathrm{R}}(t)\|_2 \leq \|\mathcal{B}(t)\|_{\mathrm{F}}\|\mathcal{B}(t)\mathbf{e}_{\mathrm{S}}(t)\|_2\\
\leq&\|\mathcal{B}(t)\|_{\mathrm{F}}^2\|\mathbf{e}_{\mathrm{S}}(t)\|_2 \leq \delta^2\|\mathbf{e}_{\mathrm{S}}(t)\|_2.
\end{aligned} \tag{23}$$

Then, the target bound of the L_2 norm of solution error $\mathbf{e}_{\mathrm{S}}(t)$ of ARKZNN model (8) is described as $\|\mathbf{e}_{\mathrm{S}}(t)\|_2 > \sigma/\delta^2$. Based on the convergence property of RKZNN model (7) for solving the temporally dependent QP problem with EC (1), we can obtain the convergence time for RKZNN model (7) arriving the target bound of the 2-norm of solution error $\mathbf{e}_{\mathrm{S}}(t)$ by the following equation:

$$\frac{1}{\sqrt{\alpha}}\|\mathbf{e}_{\mathrm{R}}(0)\|_2 \exp\left(-\frac{\eta}{2}t\right) = \frac{\sigma}{\delta^2}, \tag{24}$$

and the convergence time is

$$t_{\mathrm{c}} = \frac{2}{\eta}\ln\left(\frac{\delta^2\|\mathbf{e}_{\mathrm{R}}(0)\|_2}{\sigma\sqrt{\alpha}}\right).$$

Therefore, the L_2 norm of solution error $\mathbf{e}_{\mathrm{S}}(t)$ of RKZNN model (7) continuously, exponentially, and globally converges to the upper bounded σ/δ^2 for unified linear system (4) with exponential rate $\eta/2$, and the convergence time is less than $2\ln(\delta^2\|\mathbf{e}_{\mathrm{R}}(0)\|_2/\sigma\sqrt{\alpha})/\eta$. Moreover, the ARKZNN model (8) is finite time bounded convergent to the theoretical solution $\mathbf{y}^*(t)$ of unified linear system (4), which also approximates the theoretical solution $\mathbf{x}^*(t)$ of the temporally dependent QP problem with EC (1) in an acceptable range. □

Remark 4: Theoretically, the target for solving the temporally dependent QP problem with EC (1) is that the residual error $\mathbf{e}_{\mathrm{R}}(t)$ of unified linear system (4) should converge to zero. Since the denominator of the RKZNN model (7) can be expressed as $\mathbf{e}_{\mathrm{R}}^{\mathrm{T}}(t)\mathcal{B}(t)\mathcal{B}^{\mathrm{T}}(t)\mathbf{e}_{\mathrm{R}}(t)$, the descent property of the RKZNN model (7) may be suffered with the singularity problem. In order to deal with this singularity problem, we set a rigid threshold $\sigma \in \mathbb{R}^+$ to avoid non-steady blowing-up states. Inspired by the definition of limitation presented by Cauchy, we show that the ARKZNN model (8) can reach the linear bound related with any rigid threshold $\sigma > 0$ in a finite time, which implies that the ARKZNN model (8) should be adopted to obtain an approximate solution for the solving the temporally dependent QP problem with EC (1) in any precision. Fig. 3 illustrates the convergence process of the ARKZNN model (8) for solving the temporally dependent QP problem with EC (1).

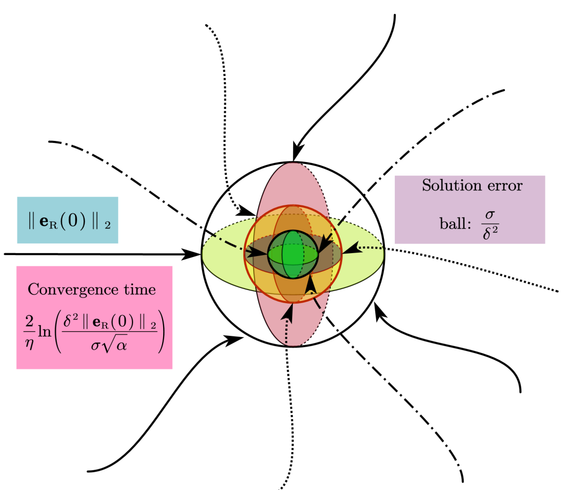

Fig. 3. Convergence process of ARKZNN model (8) for solving temporally dependent QP problem with EC (1).

In addition, we give the convergence properties of the ARKZNN model without PF (9) and the ARKZNN model without DF (10) by the following two theorems.

Theorem 3: Suppose that the temporally dependent matrix $\mathcal{B}(t)$ is differentiable with order-2 and satisfies $\|\mathcal{B}(t)\|_{\mathrm{F}} \leq \delta$, and the temporally dependent $\mathbf{m}(t)$ is differentiable with the second order. Starting with initial vector $\mathbf{y}(0)$ and for any $\sigma > 0$, there exists a constant c, such that the steady-state residual error of the ARKZNN model without DF (10) for solving the unified linear system (4) satisfies $\|\mathcal{B}(t)\mathbf{y}(t) - \mathbf{m}(t)\|_2 = c$ for any $t \in [0, +\infty)$.

Proof. The convergence property of the ARKZNN model without DF (10) for solving the unified linear system (4) comes from the convergence property of the RKZNN model without DF, which is given details in Appendix. □

Theorem 4: Suppose that the temporally dependent matrix $\mathcal{B}(t)$ is differentiable with order-2 and satisfies $\|\mathcal{B}(t)\|_{\mathrm{F}} \leq \delta$, and the temporally dependent $\mathbf{m}(t)$ is differentiable with order-2 and satisfies $\|\mathbf{m}(t)\|_2 \leq \gamma$. Besides, the time derivative matrix $\dot{\mathcal{B}}(t)$ and the time derivative vector $\dot{\mathbf{m}}(t)$ are bounded and satisfies $\|\dot{\mathcal{B}}(t)\|_{\mathrm{F}} \leq \xi$ and $\|\dot{\mathbf{m}}(t)\|_2 \leq \omega$. Starting with initial vector $\mathbf{y}(0)$ and for any $\sigma > 0$, the steady-state solution error bound of the ARKZNN model without DF (10) for solving the theoretical solution $\mathbf{y}^*(t)$ of the unified linear system (4) is formulated as

$$\frac{\sigma}{\delta^2} < \lim_{t\to\infty}\|\mathbf{y}(t) - \mathbf{y}^*(t)\|_2 \leq \frac{2\delta\xi\gamma + 2\alpha\omega}{\sqrt{\alpha}(\alpha\eta - 2\delta\xi)}, \tag{25}$$

where the ARKZNN design parameter η should be large enough, and $\alpha > 0 \in \mathbb{R}$ is the infimum of the set of minimal positive eigenvalues of $\mathcal{B}^{\mathrm{T}}(t)\mathcal{B}(t)$.

Proof. The convergence property of the ARKZNN model without PF (9) for solving the unified linear system (4) comes from the convergence property of the RKZNN model without PF, which is given details in Appendix. □

V. Numerical Experiment and Discussion

In this section, we conduct a numerical experiment to show the validity, integration, and superiority of the presented ARKZNN model (8) for solving the temporally dependent QP problem with EC (1).

A. Experiment Formulation and Setup

In this section, we firstly consider a temporally dependent QP problem with EC, which is described by the following optimization problem:

$$\begin{aligned}\min_{\mathbf{x}(t)}.\ & (\sin(t)+2)(x_1^2(t)+x_2^2(t)) + 2\cos(t)x_1(t)x_2(t)\\ & -\sin(t)x_1(t) - \cos(t)x_2(t),\\ \text{s.t.}\ & \sin(t)x_1(t) + \cos(t)x_2(t) = \sin(t),\end{aligned} \tag{26}$$

where $\mathbf{x}(t) = [x_1(t), x_2(t)]^{\mathrm{T}}$, and $t \in [0, T)$. Based on the Lagrange multiplier method, the above temporally dependent QP problem with EC (26) is transformed into the unified linear

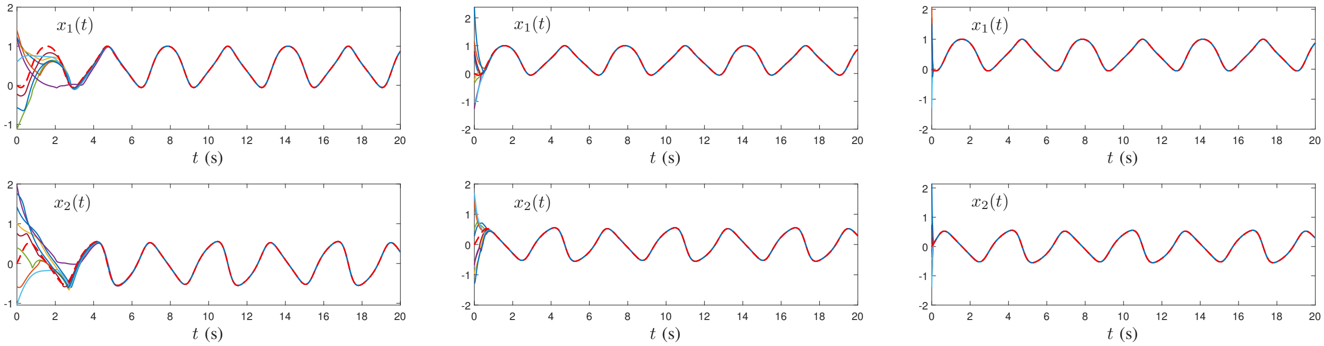

(a) (b) (c)

Fig. 4. Experiment results synthesized by ARKZNN model (8) for solving temporally dependent QP problem with EC (26) with different Zhang design parameters. Specifically, (a) comparison result of model solutions and theoretical solutions synthesized by ARKZNN model (8) with Zhang design parameter $\eta = 1$. (b) Comparison result of model solutions and theoretical solutions synthesized by ARKZNN model (8) with Zhang design parameter $\eta = 5$. (c) Comparison result of model solutions and theoretical solutions synthesized by ARKZNN model (8) with Zhang design parameter $\eta = 20$.

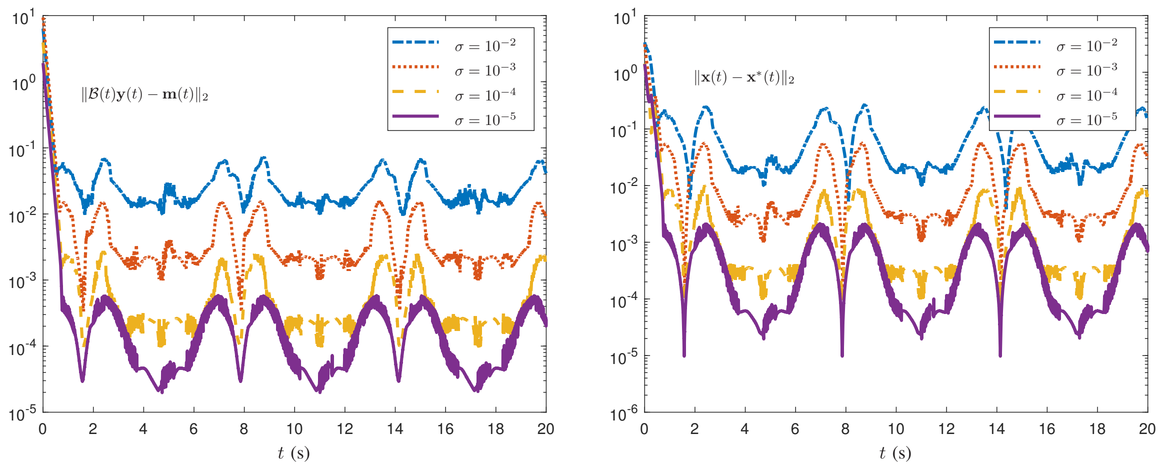

(a) (b)

Fig. 5. Experiment results synthesized by ARKZNN model (8) for solving temporally dependent QP problem with EC (26) with different rigid threshold parameters. Specifically, (a) comparison results of residual errors synthesized by ARKZNN model (8) with rigid threshold parameters $\sigma = 10^{-2}, 10^{-3}, 10^{-4}$, and 10^{-5}. (b) Comparison results of solution errors synthesized by ARKZNN model (8) with rigid threshold parameters $\sigma = 10^{-2}, 10^{-3}, 10^{-4}$, and 10^{-5}.

equation (4), whose coefficients are given by the following temporally dependent matrix and temporally dependent vector:

$$\mathcal{B}(t) = \begin{bmatrix} \sin(t)+2 & \cos(t) & \sin(t) \\ \cos(t) & \sin(t)+2 & \cos(t) \\ \sin(t) & \cos(t) & 0 \end{bmatrix},$$
$$\mathbf{y}(t) = \begin{bmatrix} x_1(t) \\ x_2(t) \\ l(t) \end{bmatrix}, \mathbf{m}(t) = \begin{bmatrix} \sin(t) \\ \cos(t) \\ \sin(t) \end{bmatrix},$$

where $l(t)$ is the corresponding Lagrange multiplier parameter.

We use the above temporally dependent QP problem with EC (26) to check the parameters influence and convergence property of our proposed ARKZNN model (8). The related numerical experiments are conducted on the simulation platform relying on the MATLAB R2022a on a PC to present the parameters influence and convergence property of the proposed ARKZNN model (8) for solving the temporally dependent QP problem with EC. The hardware environment of these numerical experiments is a laptop with Intel (R) Core (TM) i7-7700HQ CPU (2.80 GHz) and 8.00 GB RAM.

B. Parameters Influence of ARKZNN Model

In this subsection, we analyse the influence of the Zhang design parameter and threshold parameter on the ARKZNN model (8) for solving the temporally dependent QP problem with EC.

1) Zhang design parameter influence of ARKZNN model: From the expression of (8), we can see that the Zhang design parameter η plays an important role on the convergence speed of the ARKZNN model for solving the temporally dependent QP problem with EC. In detail, Theorem 1 shows that the convergence rate of RKZNN model (7) is positive proportional to the Zhang design parameter η. In order to visualize influence of the Zhang design parameter on ARKZNN model, we adopt the ARKZNN model (8) with different Zhang design parameters η to solve the problem of temporally dependent QP with EC (26). In these numerical experiments, we set the simulation duration T as 20 s, and the rigid threshold σ as 10^{-5}. Besides, we use Matlab toolbox **ode45** with the same function settings to obtain the solution of the ARKZNN model (8) with different Zhang design parameters η. In Fig. 4, we illustrate the solutions of the ARKZNN model (8) and the theoretical solution, where the solid lines represent the element-wise solutions of the ARKZNN model (8) with different Zhang design parameters η and eight random initial states $\mathbf{y}(0)$, and the dashed lines represent the element-wise theoretical solution of the temporally dependent QP problem with EC (26). From Fig. 4, we can see that the solutions of the ARKZNN model (8) with different Zhang design parameters η are consistent with the theoretical solution of the temporally dependent QP problem with EC (26) after these models arrive at steady-state, which implies that the ARKZNN model (8) can be adopted to solve the problem of the temporally dependent QP with EC (26) very well even for small Zhang design parameters η. Moreover, as the Zhang design parameter η increases, the convergence time decreases. This fact substantiates the relationship of Zhang design parameter η and the convergence speed of RKZNN model (7) described in Theorem 1.

2) Rigid threshold parameter influence of ARKZNN model: From Theorem 2, we can see that the upper bound of $\|\mathbf{e}_\mathrm{S}\|_2$ of the ARKZNN model (8) with the rigid threshold σ for solving temporally dependent QP problem with EC is σ/δ^2, which implies that this upper bound is positive proportional to the rigid threshold σ. Moreover, we can obtain the upper bound of $\|\mathbf{e}_\mathrm{R}\|_2$ of the ARKZNN model (8) with the rigid threshold σ for solving temporally dependent QP problem with EC is σ/δ, which implies that this upper bound is also positive proportional to the rigid threshold σ. In order to visualize influence of the rigid threshold parameter on ARKZNN model, we adopt the ARKZNN model (8) with different rigid threshold parameters σ to solve the problem of temporally dependent QP with EC (26). In these numerical experiments, we set the simulation duration T as 20 s, and the Zhang design parameter η as 5. Besides, we use Matlab toolbox **ode45** with the same function settings to obtain the solution of the ARKZNN model (8) with different rigid threshold parameters σ. In Fig. 5, we illustrate the comparison results of residual errors $\|\mathcal{B}(t)\mathbf{y}(t)-\mathbf{m}(t)\|_2$ synthesized by the ARKZNN model (8) for solving the temporally dependent QP problem with EC (26) with rigid threshold parameters $\sigma = 10^{-2}$, 10^{-3}, 10^{-4}, and 10^{-5}. From Fig. 5, we can see that $\|\mathbf{e}_\mathrm{S}\|_2$ and $\|\mathbf{e}_\mathrm{R}\|_2$ are decreasing, when the rigid threshold σ decreases. This fact substantiates the positive proportional relationships of the upper bound of $\|\mathbf{e}_\mathrm{S}\|_2$ and $\|\mathbf{e}_\mathrm{R}\|_2$ with the rigid threshold σ. Moreover, as the rigid threshold σ decreases, the convergence time increases. This fact substantiates the relationship of rigid threshold σ and the bounded convergence time of RKZNN model (7) described in Theorem 2.

C. Ablation Experiments

In this subsection, we conduct an ablation experiment to show the important of the whole AKRZNN model (8). In detail, we adopt the ARKZNN model (8), ARKZNN model without PF (9), and ARKZNN model without DF (10) to solve the problem of temporally dependent QP with EC (26). In this ablation experiment, we set the simulation duration T as 20 s, the Zhang design parameter η as 5, and the rigid threshold σ as 10^{-5}. Besides, we use Matlab toolbox **ode45** with the same function settings to obtain the solutions of the ARKZNN model (8), ARKZNN model without PF (9), and ARKZNN model without DF (10). In Fig. 6, we illustrate the comparison results of residual errors $\|\mathcal{B}(t)\mathbf{y}(t)-\mathbf{m}(t)\|_2$ synthesized by the ARKZNN model (8), ARKZNN model without PF (9), and ARKZNN model without DF (10) for solving the temporally dependent QP problem with EC (26). From Fig. 6, we can see that the residual error synthesized by the ARKZNN model without PF (9) stays at a constant level, which substantiates its convergence property described in Theorem 3. In addition, the residual error synthesized by the ARKZNN model without DF (10) closes to zero in certain range, which substantiates its convergence property in the proof of Theorem 4. More importantly, the ARKZNN model (8) has the best performance among these three models for solving the temporally dependent QP problem with EC (26). This ablation experiment shows that the interaction of the PF and DF terms makes the ARKZNN model (8) obtain the high precision solution of the problem of the temporally dependent QP with EC (26).

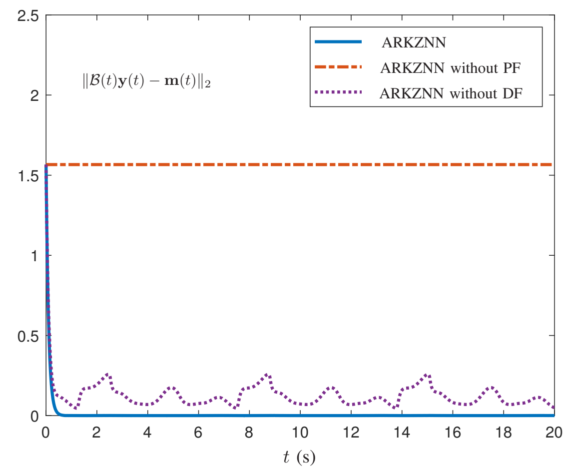

Fig. 6. Comparison results of residual errors synthesized by ARKZNN model (8), ARKZNN model without PF (9), and ARKZNN model without DF (10) for solving temporally dependent QP problem with EC (26).

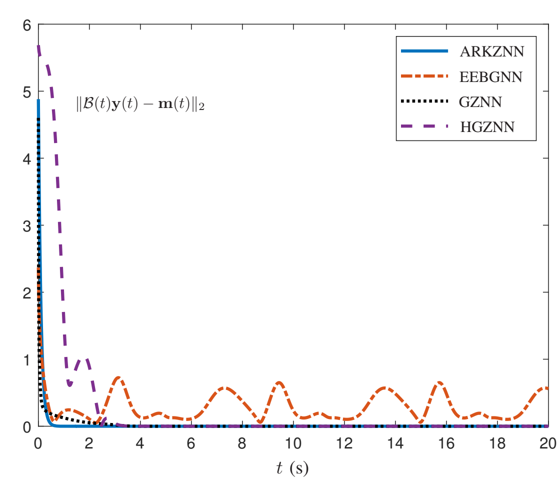

Fig. 7. Comparison results of residual errors synthesized by by ARKZNN model (8), EEBGNN model (11), HGZNN model (12) and GZNN model (13) for solving temporally dependent QP problem with EC (26)

D. Overall Performance

In this subsection, we conduct a comparison experiment to show the superiority of the AKRZNN model (8). In detail, we adopt the ARKZNN model (8), EEBGNN model (11), HGZNN model (12), and GZNN model (13) to solve the problem of temporally dependent QP with EC (26). The 2-norm of the residual error $\|\mathcal{B}(t)\mathbf{y}(t) - \mathbf{m}(t)\|_2$ is used to assess the performance of these models. In this comparison experiment, we set the simulation duration T as 20 s, the QP related design parameters η, κ, and υ as 10, and the rigid threshold σ as 10^{-5}. Besides, we use Matlab toolbox **ode45** with the same function settings to obtain the solution of the ARKZNN model (8), EEBGNN model (11), HGZNN model (12), and GZNN model (13). In Fig. 7, we illustrate the comparison results of residual errors $\|\mathcal{B}(t)\mathbf{y}(t) - \mathbf{m}(t)\|_2$ synthesized by the ARKZNN model (8), EEBGNN model (11), HGZNN model (12), and GZNN model (13) for solving the temporally dependent QP problem with EC (26). From Fig. 7, we can see that the ARKZNN model (8) has the best performance among these four models for solving the temporally dependent QP problem with EC (26).

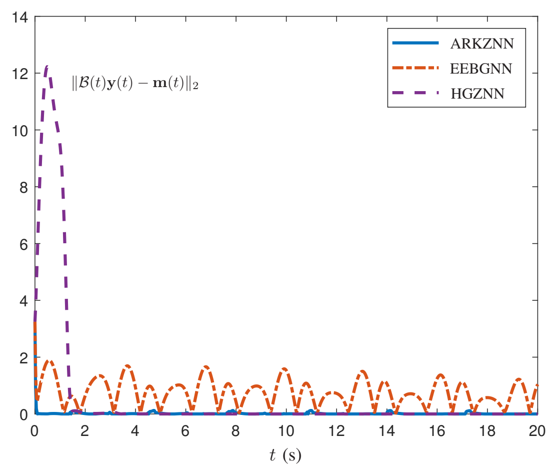

Fig. 8. Comparison results of residual errors synthesized by by ARKZNN model (8), EEBGNN model (11), and HGZNN model (12) for solving temporally dependent QP problem with EC (27)

E. Example with Hybrid Function Coefficients

In this subsection, we consider a complex temporally dependent QP problem with EC, which is described by the following optimization problem:

$$\begin{aligned}\min_{\mathbf{x}(t)}.\ &(\sin(2t)+2.5)(x_1^2(t)+x_2^2(t)) + \frac{2}{t+1}x_1(t)x_2(t)\\ &-2\sin(t)x_1(t) - 3\cos(2t)x_2(t),\\ \text{s.t.}\ &\ln(1+0.1t)x_1(t)+\sin(t)x_2(t) = 2\sin(3t),\end{aligned} \tag{27}$$

where $\mathbf{x}(t) = [x_1(t), x_2(t)]^{\mathrm{T}}$, and $t \in [0, T)$. Since the GZNN model causes the singularity problem, we adopt the ARKZNN model (8), EEBGNN model (11), and HGZNN model (12) to solve the problem of temporally dependent QP with EC (27). The 2-norm of the residual error $\|\mathcal{B}(t)\mathbf{y}(t) - \mathbf{m}(t)\|_2$ is used to assess the performance of these models. In this comparison experiment, we set the simulation duration T as 20 s, the QP related design parameters η, κ, and υ as 50, and the rigid threshold σ as 10^{-5}. Besides, we use Matlab toolbox **ode45** with the same function settings to obtain the solutions of the ARKZNN model (8), EEBGNN model (11), and HGZNN model (12). In Fig. 8, we illustrate the comparison results of residual errors $\|\mathcal{B}(t)\mathbf{y}(t) - \mathbf{m}(t)\|_2$ synthesized by ARKZNN model (8), EEBGNN model (11), and HGZNN model (12) for solving the temporally dependent QP problem with EC (27). From Fig. 8, we can see that the ARKZNN model (8) has the best performance among these three models for solving the temporally dependent QP problem with EC (27).

Algorithm 1 Euler-ARKZNN algorithm for solving robot arm path-tracking problem.

Data:
Task duration T, sampling gap g, initial joint angles vector $\mathbf{a}_0$, parameters τ and $\hat{\tau}$, and initial states $\mathbf{y}_0$, $\dot{\mathcal{B}}_0$, and $\dot{\mathbf{m}}_0$
Result: Joint angles vector $\mathbf{a}_{k+1}$
while $k = 1 : \lceil \frac{T}{g} \rceil$
  if $\|\varepsilon_k\|_2 > \sigma$
    Get $\mathcal{B}_k, \mathbf{m}_k$, and $\mathbf{y}_k$
    $\dot{\mathcal{B}}_k \leftarrow (\mathcal{B}_k - \mathcal{B}_{k-1})/g$
    $\dot{\mathbf{m}}_k \leftarrow (\mathbf{m}_k - \mathbf{m}_{k-1})/g$
    Compute $\mathbf{y}_{k+1}$ by Euler-ARKZNN algorithm (15)
  else
    $\mathbf{y}_{k+1} = \mathbf{y}_k$
  end if
  $\dot{\mathbf{a}}_{k+1} = \mathbf{y}_{k+1}(1:6)$
  $\mathbf{a}_{k+1} = g\dot{\mathbf{a}}_{k+1} + \mathbf{a}_k$
  $k \leftarrow k+1$
end while

VI. Application to Robot Arm

In this section, we adopt the proposed Euler-ARKZNN algorithm (15) and (16) to deal with the path-tracking problem of PUMA560 robot arm.

As mentioned in our previous works, the path-tracking problem of robot arm can be formulated as the following FQP problem with EC in each future interval $[t_k, t_{k+1})$:

$$\begin{aligned}\min_{\dot{\mathbf{a}}_{k+1}}\ &\frac{1}{2}\dot{\mathbf{a}}_{k+1}^{\mathrm{T}} I_{k+1}\dot{\mathbf{a}}_{k+1} + \tau\dot{\mathbf{a}}_{k+1}^{\mathrm{T}}(\mathbf{a}_{k+1} - \mathbf{a}_0),\\ \text{s.t.}\ &J(\mathbf{a}_{k+1})\dot{\mathbf{a}}_{k+1} = \dot{\mathbf{p}}_{k+1}^{\mathrm{d}} - \hat{\tau}(f(\mathbf{a}_{k+1}) - \mathbf{p}_{k+1}^{\mathrm{d}}),\end{aligned} \tag{28}$$

where $\mathbf{a}_{k+1}$, $\dot{\mathbf{a}}_{k+1} \in \mathbb{R}^n$ denote the joint angle vector and joint velocity vector, respectively, $I_{k+1} \in \mathbb{R}^{n\times n}$ is the identity matrix, $\tau \in \mathbb{R}^+$ denotes the trade-off model parameter, $J(\mathbf{a}_{k+1}) = \partial f(\mathbf{a}_{k+1})/\partial \mathbf{a}_{k+1} \in \mathbb{R}^{m\times m}$ denotes the Jacobian matrix of robot arm, $\mathbf{p}_{k+1}^{\mathrm{d}} \in \mathbb{R}^m$ denotes the desired path, $\dot{\mathbf{p}}_{k+1}^{\mathrm{d}} \in \mathbb{R}^m$ denotes the desired end-effector velocity vector, and $\tilde{\mu} \in \mathbb{R}^+$ is the Zhang design parameter. In order to use the ARKZNN model, we rewrite the matrix and vectors of the above path-tracking problem of robot arm as follows:

$$\mathcal{B}_{k+1} = \begin{bmatrix} I_{k+1} & J^{\mathrm{T}}(\mathbf{a}_{k+1}) \\ J(\mathbf{a}_{k+1}) & O \end{bmatrix}, \mathbf{y}_k = \begin{bmatrix} \dot{\mathbf{a}}_{k+1} \\ \boldsymbol{\lambda}_{k+1} \end{bmatrix},$$

$$\mathbf{m}_k = \begin{bmatrix} -\tau(\mathbf{a}_{k+1} - \mathbf{a}_0) \\ \dot{\mathbf{p}}_{k+1}^{\mathrm{d}} - \hat{\tau}(f(\mathbf{a}_{k+1}) - \mathbf{p}_{k+1}^{\mathrm{d}}) \end{bmatrix}.$$

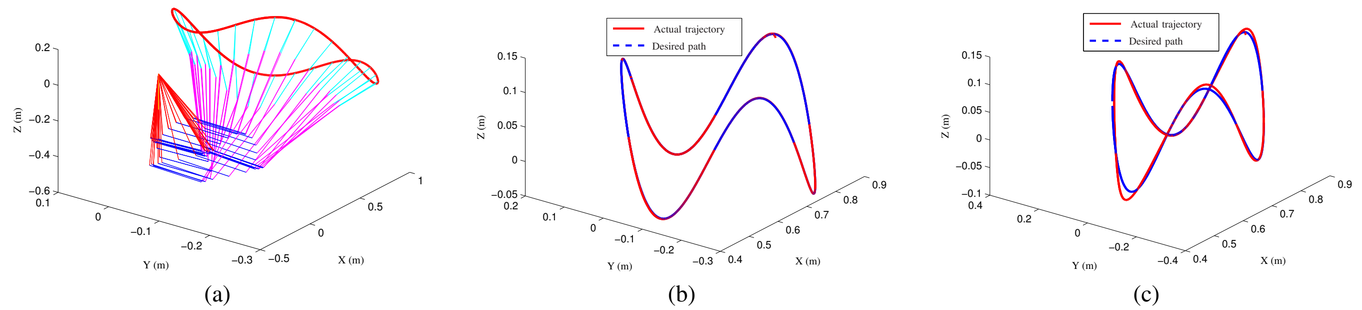

Fig. 9. Experiment results synthesized by Euler-ARKZNN and Euler-EEBGNN algorithms for solving the path-tracking problem of PUMA560. Specifically, (a) robot arm trajectory of PUMA560 synthesized by Euler-ARKZNN algorithm (15) and (16) with $\eta = 200$ and $g = 0.001$ s; (b) Desired path and end-effector trajectory synthesized by Euler-ARKZNN algorithm (15) and (16) with $\eta = 200$ and $g = 0.001$ s; (c) Desired path and end-effector trajectory synthesized by Euler-EEBGNN algorithm with $\eta = 200$ and $g = 0.001$ s.

The pseudo-code of Euler-ARKZNN algorithm for solving the robot arm path-tracking problem (28) is illustrated in Algorithm 1.

The proposed Euler-ARKZNN algorithm (15) and (16) is used to solve the above path-tracking problem (28) of PUMA560 for the following desired path:

$$\mathbf{p}_k = \begin{bmatrix} 0.2\cos(0.25\pi t_k) + \varsigma_1 \\ 0.2\sin(0.25\pi t_k) + \varsigma_2 \\ 0.09\cos(0.75\pi t_k) + 1.5 + \varsigma_3 \end{bmatrix},$$

where $\varsigma = [\varsigma_1, \varsigma_2, \varsigma_3]^{\mathrm{T}}$ is the initial point of PUMA560. In this simulation, the duration time is set as 20 s, and the sampling gap is set as 0.001 s. The initial joint angle vector is set as $\mathbf{a}_0 = [0, -0.7853.0, -1.5707, 0, -0.7853]^{\mathrm{T}}$. The model parameters and algorithm parameter are set as $\tau = 0.1$, $\hat{\tau} = 30$, and $\eta = 100$. We illustrate the robot arm trajectory of PUMA560 synthesized by Euler-ARKZNN algorithm (15) and (16) in Fig. 9(a), and the corresponding end-effector trajectory and desired path in Fig. 9(b). From Fig. 9(a) and Fig. 9(b), we can see that the proposed Euler-ARKZNN algorithm (15) and (16) can conduct the desired path-tracking task very well. As a comparison, we also tackle the same task by the Euler-EEBGNN algorithm with $\kappa = 100$, and the corresponding end-effector trajectory and desired path are illustrated in Fig. 9(c), which shows that the Euler-EEBGNN algorithm can not accomplish the desired path-tracking task. The comparison residual errors synthesized by Euler-ARKZNN and Euler-EEBGNN algorithms for solving the path-tracking problem of PUMA560 are presented in Fig. 10, which shows the validity and superiority of the proposed Euler-ARKZNN algorithm.

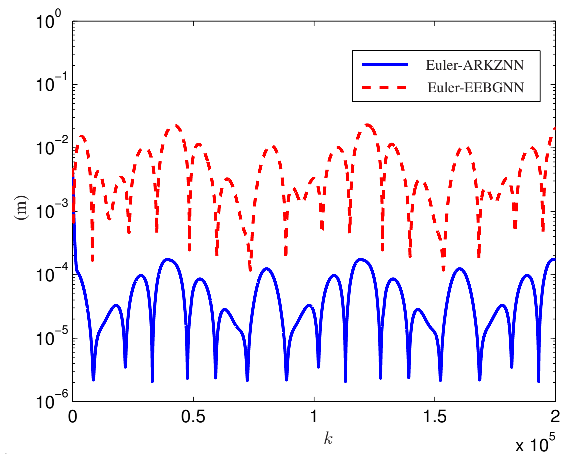

Fig. 10. Comparison results of residual errors synthesized by Euler-ARKZNN and Euler-EEBGNN algorithms for solving the path-tracking problem of PUMA560 with $\eta = \kappa = 200$ and $g = 0.001$ s.

VII. Conclusion

In this paper, a novel single total inverse-free ARKZNN model has been proposed by using the 2-norm energy cost function for solving temporally dependent QP problem with EC. The convergence properties of RKZNN and ARKZNN models have been given by Lyapunov stability theory and the thinking of limitation definition, and the parts effect of derivative feedforward and proportional feedback have been clearly described by Lyapunov stability theory and matrix spectral theory. Moreover, two numerical experiments have shown the effectiveness and superiority of ARKZNN model for solving temporally dependent QP problem with EC. Finally, the effectiveness and superiority of Euler-ARKZNN algorithm has been shown, when it has been adopted to solve the problem of robot arm path-tracking. Expanding the ARKZNN framework into the temporally dependent QP problem with IEC or the temporally dependent matrix equation solving is our future research direction.

Appendix
Proof of Theorem 3

Suppose that $\mathbf{y}^*(t)$ is the theoretical solution of unified linear system (4), that is, $\mathcal{B}(t)\mathbf{y}^*(t) = \mathbf{m}(t)$. In order to obtain the convergence property of RKZNN model without PF, we define the related residual error based Lyapunov candidate function as $\mathcal{V}_1(t) = \|\mathbf{e}_{\mathrm{R}}(t)\|_2^2/2$, which is a positive-definite bilinear temporally dependent function. Then, the derivative of Lyapunov candidate function $\mathcal{V}_1(t)$ is computed as follows:

$$\begin{aligned} \dot{\mathcal{V}}_1(t) =& \frac{\mathrm{d}}{\mathrm{d}t}\left(\frac{\|\mathbf{e}_{\mathrm{R}}(t)\|_2^2}{2}\right) = \mathbf{e}_{\mathrm{R}}^{\mathrm{T}}(t)\dot{\mathbf{e}}_{\mathrm{R}}(t) \\ =& \mathbf{e}_{\mathrm{R}}^{\mathrm{T}}(t)(\dot{\mathcal{B}}(t)\mathbf{y}(t) + \mathcal{B}(t)\dot{\mathbf{y}}(t) - \dot{\mathbf{m}}(t)) \\ =& \mathbf{e}_{\mathrm{R}}^{\mathrm{T}}(t)\Big(-\mathcal{B}(t)\frac{\boldsymbol{\varepsilon}(t)\mathbf{e}_{\mathrm{R}}^{\mathrm{T}}(t)(\dot{\mathcal{B}}(t)\mathbf{y}(t) - \dot{\mathbf{m}}(t))}{\|\boldsymbol{\varepsilon}(t)\|_2^2} \\ &+ \dot{\mathcal{B}}(t)\mathbf{y}(t) - \dot{\mathbf{m}}(t)\Big) = 0. \end{aligned} \tag{29}$$

That is to say, the Lyapunov candidate function $\mathcal{V}_1(t)$ satisfies the following ordinary derivative equation by (29):

$$\dot{\mathcal{V}}_1(t) = 0, \text{for any } t \in [0, +\infty).$$

Then, there exists a constant c_0, such that the Lyapunov candidate function $\mathcal{V}_1(t)$ is formulated as the following explicit form:

$$\mathcal{V}_1(t) = c_0, \text{for any } t \in [0, +\infty). \tag{30}$$

Substituting $\mathcal{V}_1(t) = \|\mathbf{e}_\mathrm{R}(t)\|_2^2/2$ into (30), we obtain the explicit form of the 2-norm of residual error $\mathbf{e}_\mathrm{R}(t)$:

$$\|\mathbf{e}_\mathrm{R}(t)\|_2 = \sqrt{2}c_0 \triangleq c, \text{for any } t \in [0, +\infty). \tag{31}$$

Thus, the proof is completed.

Proof of Theorem 4

Assume that $\mathbf{y}^*(t)$ is the theoretical solution of unified linear system (4), that is, $\mathcal{B}(t)\mathbf{y}^*(t) = \mathbf{m}(t)$. In order to obtain the convergence property of RKZNN model without DF, we define the related residual error based Lyapunov candidate function as $\mathcal{V}_2(t) = \|\mathbf{e}_\mathrm{R}(t)\|_2^2/2$, which is a positive-definite bilinear temporally dependent function. Then, the derivative of Lyapunov candidate function $\mathcal{V}_2(t)$ is computed as follows:

$$\begin{aligned}\dot{\mathcal{V}}_2(t) =& \frac{\mathrm{d}}{\mathrm{d}t}\left(\frac{\|\mathbf{e}_\mathrm{R}(t)\|_2^2}{2}\right) = \mathbf{e}_\mathrm{R}^\mathrm{T}(t)\dot{\mathbf{e}}_\mathrm{R}(t)\\ =& \mathbf{e}_\mathrm{R}^\mathrm{T}(t)(\dot{\mathcal{B}}(t)\mathbf{y}(t) + \mathcal{B}(t)\dot{\mathbf{y}}(t) - \dot{\mathbf{m}}(t))\\ =& \mathbf{e}_\mathrm{R}^\mathrm{T}(t)(\dot{\mathcal{B}}(t)\mathbf{y}(t) - \dot{\mathbf{m}}(t)) - \eta\frac{\boldsymbol{\varepsilon}^\mathrm{T}(t)\boldsymbol{\varepsilon}(t)\|\mathbf{e}_\mathrm{R}(t)\|_2^2}{2\|\boldsymbol{\varepsilon}(t)\|_2^2}\\ =& \mathbf{e}_\mathrm{R}^\mathrm{T}(t)\dot{\mathcal{B}}(t)\mathbf{y}(t) - \mathbf{e}_\mathrm{R}^\mathrm{T}(t)\dot{\mathbf{m}}(t) - \frac{\eta}{2}\|\mathbf{e}_\mathrm{R}(t)\|_2^2.\end{aligned} \tag{32}$$

In order to study the property of the Lyapunov time derivative function $\dot{\mathcal{V}}_2(t)$, we should analyze the last expression of (32) term by term. For the first term $\mathbf{e}_\mathrm{R}^\mathrm{T}(t)\dot{\mathcal{B}}(t)\mathbf{y}(t)$, we obtain the following inequality by using the Cauchy-Schwarz and the norm compatibility inequalities:

$$\begin{aligned}\mathbf{e}_\mathrm{R}^\mathrm{T}(t)\dot{\mathcal{B}}(t)\mathbf{y}(t) \leq& \|\mathbf{e}_\mathrm{R}(t)\|_2\|\dot{\mathcal{B}}(t)\|_\mathrm{F}\|\mathbf{y}(t)\|_2\\ \leq& \xi\|\mathbf{e}_\mathrm{R}(t)\|_2\|\mathbf{y}(t)\|_2.\end{aligned} \tag{33}$$

Since $\mathbf{e}_\mathrm{R}(t) = \mathcal{B}(t)\mathbf{y}(t) - \mathbf{m}(t)$, then, $\mathcal{B}(t)\mathbf{y}(t) = \mathbf{e}_\mathrm{R}(t) + \mathbf{m}(t)$. We obtain the following inequality:

$$\begin{aligned}\alpha\|\mathbf{y}(t)\|_2^2 \leq& \mathbf{y}^\mathrm{T}(t)\mathcal{B}^\mathrm{T}(t)\mathcal{B}(t)\mathbf{y}(t)\\ =& \mathbf{y}^\mathrm{T}(t)\mathcal{B}^\mathrm{T}(t)(\mathbf{e}_\mathrm{R}(t) + \mathbf{m}(t))\\ \leq& \|\mathbf{y}(t)\|_2\|\mathcal{B}(t)\|_\mathrm{F}(\|\mathbf{e}_\mathrm{R}(t)\|_2 + \|\mathbf{m}(t)\|_2).\end{aligned} \tag{34}$$

Then, we get the bounded control inequality of $\|\mathbf{y}(t)\|_2$ based on (34) as follows:

$$\|\mathbf{y}(t)\|_2 \leq \frac{\delta}{\alpha}(\|\mathbf{e}_\mathrm{R}(t)\|_2 + \gamma). \tag{35}$$

Substituting (35) into (33), we obtain the following control inequality of the first term:

$$\mathbf{e}_\mathrm{R}^\mathrm{T}(t)\dot{\mathcal{B}}(t)\mathbf{y}(t) \leq \frac{\delta\xi}{\alpha}\|\mathbf{e}_\mathrm{R}(t)\|_2(\|\mathbf{e}_\mathrm{R}(t)\|_2 + \gamma). \tag{36}$$

For the second term, we obtain the following control inequality:

$$-\mathbf{e}_\mathrm{R}^\mathrm{T}(t)\dot{\mathbf{m}}(t) \leq \|\mathbf{e}_\mathrm{R}(t)\|_2\|\dot{\mathbf{m}}(t)\|_2 \leq \omega\|\mathbf{e}_\mathrm{R}(t). \tag{37}$$

Substituting (36) and (37) into (32), we obtain the following control inequality:

$$\dot{\mathcal{V}}_2(t) \leq -\frac{\alpha\eta - 2\delta\xi}{2\alpha}\|\mathbf{e}_\mathrm{R}(t)\|_2(\|\mathbf{e}_\mathrm{R}(t)\|_2 - \frac{2\delta\xi\gamma + 2\alpha\omega}{\alpha\eta - 2\delta\xi}), \tag{38}$$

where the Zhang design parameter η should be large enough. As t evolves, $\|\mathbf{e}_\mathrm{R}(t)\|_2$ falls into the following three situations:

- **Case I**: If $\|\mathbf{e}_\mathrm{R}(t)\|_2 - (2\delta\xi\gamma + 2\alpha\omega)/(\alpha\eta - 2\delta\xi) > 0$, then $\dot{\mathcal{V}}_2(t) < 0$, which implies that $\mathbf{e}_\mathrm{R}(t)$ asymptotically converges to $\mathbf{0}$.
- **Case II**: If $\|\mathbf{e}_\mathrm{R}(t)\|_2 - (2\delta\xi\gamma + 2\alpha\omega)/(\alpha\eta - 2\delta\xi) = 0$, then $\dot{\mathcal{V}}_2(t) \leq 0$. According to **Case I**, we only need to consider the issue $\dot{\mathcal{V}}_2(t) = 0$, which makes $\|\mathbf{e}_\mathrm{R}(t)\|_2$ stay on the ball surface with radius $(2\delta\xi\gamma+2\alpha\omega)/(\alpha\eta-2\delta\xi)$.
- **Case III**: If $\|\mathbf{e}_\mathrm{R}(t)\|_2 - (2\delta\xi\gamma + 2\alpha\omega)/(\alpha\eta - 2\delta\xi) < 0$, there exists a positive constant l_0 such that $\dot{\mathcal{V}}_2(t) \leq l_0$ based on the bounded conditions of $\|\mathbf{y}(t)\|_2$, $\|\mathbf{m}(t)\|_2$, and $\mathcal{B}(t)$. According to **Case II**, we only need to consider the issue $0 < \dot{\mathcal{V}}_2(t) \leq l_0$. In this issue, $\mathcal{V}_2(t)$ is an increasing function, which also makes $\|\mathbf{e}_\mathrm{R}(t)\|_2$ as an increasing function. Therefore, there exists a time instant t_0, such that $\|\mathbf{e}_\mathrm{R}(t_0)\|_2 = 0$, which also goes back to **Case II**.

From above analyses, the upper bound of the steady-state residual error of RKZNN model without DF is formulated as:

$$\lim_{t\to+\infty}\|\mathbf{e}_\mathrm{R}(t)\|_2 \leq \frac{2\delta\xi\gamma + 2\alpha\omega}{\alpha\eta - 2\delta\xi}. \tag{39}$$

On the basis of (22), (23), and (39), we obtain the range of steady-state solution error of ARKZNN model without DF (10) as follows:

$$\frac{\sigma}{\delta^2} < \lim_{t\to+\infty}\|\mathbf{e}_\mathrm{S}(t)\|_2 \leq \frac{2\delta\xi\gamma + 2\alpha\omega}{\sqrt{\alpha}(\alpha\eta - 2\delta\xi)}. \tag{40}$$

Thus, the proof is completed.

References

[1] Z. Li, J. Deng, R. Lu, Y. Xu, J. Bai, and C.-Y. Su, “Trajectory-tracking control of mobile robot systems incorporating neural-dynamic optimized model predictive approach,” *IEEE Transactions on Systems, Man, and Cybernetics: Systems*, vol. 46, no. 6, pp. 740–749, 2016.

[2] L. Jin, Y. Zhang, S. Li, and Y. Zhang, “Modified ZNN for time-varying quadratic programming with inherent tolerance to noises and its application to kinematic redundancy resolution of robot manipulators,” *IEEE Transactions on Industrial Electronics*, vol. 63, no. 11, pp. 6978–6988, 2016.

[3] K. Rajagopal, S. N. Balakrishnan, and J. R. Busemeyer, “Neural network-based solutions for stochastic optimal control using path integrals,” *IEEE Transactions on Neural Networks and Learning Systems*, vol. 28, no. 3, pp. 534–545, 2017.

[4] M. Fazlyab, M. Morari, and G. J. Pappas, “Safety verification and robustness analysis of neural networks via quadratic constraints and semidefinite programming,” *IEEE Transactions on Automatic Control*, vol. 67, no. 1, pp. 1–15, 2022.

[5] G. Wang, J. Qiao, C. Liu, and Z. Shen, “How deep is deep enough for deep belief network for approximating model predictive control law,” *IEEE Transactions on Automation Science and Engineering*, vol. 19, no. 3, pp. 2067–2078, 2022.

[6] Z. Li, Y. Xia, C.-Y. Su, J. Deng, J. Fu, and W. He, "Missile guidance law based on robust model predictive control using neural-network optimization," *IEEE Transactions on Neural Networks and Learning Systems*, vol. 26, no. 8, pp. 1803–1809, 2015.

[7] A. Bemporad, "A quadratic programming algorithm based on nonnegative least squares with applications to embedded model predictive control," *IEEE Transactions on Automatic Control*, vol. 61, no. 4, pp. 1111–1116, 2016.

[8] Y. Leung, K.-Z. Chen, Y.-C. Jiao, X.-B. Gao, and K. S. Leung, "A new gradient-based neural network for solving linear and quadratic programming problems," *IEEE Transactions on Neural Networks*, vol. 12, no. 5, pp. 1074–1083, 2001.

[9] Y. Yang and J. Cao, "Solving quadratic programming problems by delayed projection neural network," *IEEE Transactions on Neural Networks*, vol. 17, no. 6, pp. 1630–1634, 2006.

[10] D. Arnstrm and D. Axehill, "A unifying complexity certification framework for active-set methods for convex quadratic programming," *IEEE Transactions on Automatic Control*, vol. 67, no. 6, pp. 2758–2770, 2022.

[11] S. Li, R. Kong, and Y. Guo, "Cooperative distributed source seeking by multiple robots: Algorithms and experiments," *IEEE/ASME Transactions on Mechatronics*, vol. 19, no. 6, pp. 1810–1820, 2014.

[12] S. Li, H. Wang, and M. U. Rafique, "A novel recurrent neural network for manipulator control with improved noise tolerance," *IEEE Transactions on Neural Networks and Learning Systems*, vol. 29, no. 5, pp. 1908–1918, 2018.

[13] D. Chen, Y. Zhang, and S. Li, "Tracking control of robot manipulators with unknown models: A jacobian-matrix-adaption method," *IEEE Transactions on Industrial Informatics*, vol. 14, no. 7, pp. 3044–3053, 2018.

[14] J. L. Morales, J. Nocedal, and Y. Wu, "A sequential quadratic programming algorithm with an additional equality constrained phase," *IMA Journal of Numerical Analysis*, vol. 32, no. 2, pp. 553–579, 2012.

[15] M. Mazzotti, Q. Mao, I. Bartoli, and S. Livadiotis, "A multiplicative regularized Gauss-Newton method with trust region sequential quadratic programming for structural model updating," *Mechanical Systems and Signal Processing*, vol. 131, pp. 417–433, 2019.

[16] Q. Liu and J. Wang, "A projection neural network for constrained quadratic minimax optimization," *IEEE Transactions on Neural Networks and Learning Systems*, vol. 26, no. 11, pp. 2891–2900, 2015.

[17] Y. Xia, J. Wang, and W. Guo, "Two projection neural networks with reduced model complexity for nonlinear programming," *IEEE Transactions on Neural Networks and Learning Systems*, vol. 31, no. 6, pp. 2020–2029, 2020.

[18] J. Li, Y. Shi, and H. Xuan, "Unified model solving nine types of time-varying problems in the frame of zeroing neural network," *IEEE Transactions on Neural Networks and Learning Systems*, vol. 32, no. 5, pp. 1896–1905, 2021.

[19] J. Wang, J. Wang, and Q.-L. Han, "Multivehicle task assignment based on collaborative neurodynamic optimization with discrete Hopfield networks," *IEEE Transactions on Neural Networks and Learning Systems*, vol. 32, no. 12, pp. 5274–5286, 2021.

[20] Y. Zhang, Y. Yang, and G. Ruan, "Performance analysis of gradient neural network exploited for online time-varying quadratic minimization and equality-constrained quadratic programming," *Neurocomputing*, vol. 74, no. 10, pp. 1710–1719, 2011.

[21] S. Qin, X. Le, and J. Wang, "A neurodynamic optimization approach to bilevel quadratic programming," *IEEE Transactions on Neural Networks and Learning Systems*, vol. 28, no. 11, pp. 2580–2591, 2017.

[22] Y. Zhang, H. Gong, M. Yang, J. Li, and X. Yang, "Stepsize range and optimal value for Taylor-Zhang discretization formula applied to zeroing neurodynamics illustrated via future equality-constrained quadratic programming," *IEEE Transactions on Neural Networks and Learning Systems*, vol. 30, no. 3, pp. 959–966, 2019.

[23] J. Guo and Y. Zhang, "Stepsize interval confirmation of general four-step DTZN algorithm illustrated with future quadratic programming and tracking control of manipulators," *IEEE Transactions on Systems, Man, and Cybernetics: Systems*, vol. 51, no. 3, pp. 1662–1670, 2021.

[24] Y. Zhang, D. Jiang, and J. Wang, "A recurrent neural network for solving Sylvester equation with time-varying coefficients," *IEEE Transactions on Neural Networks*, vol. 13, no. 5, pp. 1053–1063, 2002.

[25] Y. Zhang, X. Li, and Z. Li, "Modeling and verification of Zhang neural networks for online solution of time-varying quadratic minimization and programming," in *Advances in Computation and Intelligence*. Berlin, Heidelberg: Springer Berlin Heidelberg, 2009, pp. 101–110.

[26] Y. Yang and Y. Zhang, "Superior robustness of power-sum activation functions in Zhang neural networks for time-varying quadratic programs perturbed with large implementation errors," *Neural Comput. Appl.*, vol. 22, no. 1, pp. 175–185, 2013.

[27] L. Xiao, S. Li, J. Yang, and Z. Zhang, "A new recurrent neural network with noise-tolerance and finite-time convergence for dynamic quadratic minimization," *Neurocomputing*, vol. 285, pp. 125–132, 2018.

[28] Z. Zhang, L.-D. Kong, and L. Zheng, "Power-type varying-parameter RNN for solving TVQP problems: Design, analysis, and applications," *IEEE Transactions on Neural Networks and Learning Systems*, vol. 30, no. 8, pp. 2419–2433, 2019.

[29] Y. Qi, L. Jin, Y. Wang, L. Xiao, and J. Zhang, "Complex-valued discrete-time neural dynamics for perturbed time-dependent complex quadratic programming with applications," *IEEE Transactions on Neural Networks and Learning Systems*, vol. 31, no. 9, pp. 3555–3569, 2020.

[30] L. Jia, L. Xiao, J. Dai, Z. Qi, Z. Zhang, and Y. Zhang, "Design and application of an adaptive fuzzy control strategy to zeroing neural network for solving time-variant QP problem," *IEEE Transactions on Fuzzy Systems*, vol. 29, no. 6, pp. 1544–1555, 2021.

[31] Z. Zhang, Z. Li, and S. Yang, "A barrier varying-parameter dynamic learning network for solving time-varying quadratic programming problems with multiple constraints," *IEEE Transactions on Cybernetics*, vol. 52, no. 9, pp. 8781–8792, 2022.

[32] Y. Zhang, Y. Ling, M. Yang, S. Yang, and Z. Zhang, "Inverse-free discrete ZNN models solving for future matrix pseudoinverse via combination of extrapolation and ZeaD formulas," *IEEE Transactions on Neural Networks and Learning Systems*, vol. 32, no. 6, pp. 2663–2675, 2021.